PHYSICAL REVIEW A **98**, 022518 (2018)

Calculation of atomic spectra and transition amplitudes for the superheavy element Db (Z =105)

B. G. C. Lackenby,[1] V. A. Dzuba,[1] and V. V. Flambaum[1,2]
[1]*School of Physics, University of New South Wales, Sydney 2052, Australia*
[2]*Johannes Gutenberg-Universität Mainz, 55099 Mainz, Germany*

(Received 22 April 2018; published 28 August 2018)

Atomic spectra and other properties of superheavy element dubnium (Db, $Z = 105$) are calculated using recently developed method combining configuration interaction with perturbation theory [the CIPT method, V. A. Dzuba, J. C. Berengut, C. Harabati, and V. V. Flambaum, Phys. Rev. A **95**, 012503 (2017)]. These include energy levels for low-lying states of Db and Db II, electric dipole transition amplitudes between the ground state and low-lying states of opposite parity, isotope shift for these transitions, and the ionization potential of Db. Similar calculations for Ta, which is a lighter analog of Db, are performed to control the accuracy of the calculations.

DOI: 10.1103/PhysRevA.98.022518

I. INTRODUCTION

The study of super heavy elements (SHE), $Z > 100$, has been an important field in atomic and nuclear physics for the past century [1,2]. These exotic elements, which are not found in nature, are interesting particularly in relation to the existence of the "island of stability" where stable SHE isotopes are expected to be found as predicted by theoretical nuclear shell models [2–5]. The theoretical study of SHE by means of atomic physics provides an opportunity to study the interplay between correlation and relativistic effects in extreme conditions of heavy many-electron system.

Experimental knowledge of SHEs is still limited due to difficulties caused by short lifetimes and low production rates. While elements up to Z=118 have been synthesized, the heaviest elements for which experimental spectroscopic data are available are No ($Z = 102$) and Lr ($Z = 103$). The ${}^1S_0 \rightarrow {}^1P_1^{\mathrm{o}}$ excitation energy of No ($Z = 102$) [6] and ionisation potentials (IP) of No [6] and Lr ($Z = 103$) [7] have been recently measured. The development and refinement of laser spectroscopy techniques make future measurements in the SHE region promising [8–10]. The theoretical results presented here will facilitate future experiments.

There has been significant theoretical study of SHEs with a small number of electrons (holes) above (below) closed shells. These calculations were performed using well-established many-body techniques such as couple-cluster methods [11,12], configuration interaction and many body perturbation theory (CI + MBPT) [13], correlation potential (CP) methods [14] and multiconfigurational Dirac-Fock (MCDF) [15], and so on. For SHEs $Z = 102, 103, 104$ which have 2, 3, and 4 valence electrons above the closed $5f$ shell, their spectra, ionization potentials and static polarizabilities were calculated [16–26]. Similarly, atomic properties of SHEs $Z = 112$–118 using coupled-cluster methods [27–35], CI + MBPT methods [13,36], and MCDF methods [37,38] have been calculated. Elements Mc to Og ($Z = 115$–118) have more than three external electrons and theoretical study is limited to calculation of IPs, polarizabilities, electron affinities, and so on, but not energy levels (see, e.g., Ref. [31]). Atomic properties of elements with $Z = 119$–122, which also have simple electron structure, having from one to four valence electrons, have also been theoretically studied [25,39–47]. A review of SHE atomic calculations can be found in Refs. [25,48].

While established numerical methods have been used for SHEs with relatively simple atomic structure, difficulties arise for more than four valences electrons in the open subshells in many-electron atoms ($Z = 105$–111) due to the extremely large CI basis which leads to the CI matrix of unmanageable size. This has limited the calculations mostly to ionization potentials and electric polarizabilites [49–52]. A recently developed method combining configuration interaction with perturbation theory (the CIPT method [53]) overcomes these limitations, allowing the calculation of spectra for the rest of SHE. In this work we calculate the atomic spectra of homologues Ta I and Db I, which both have five valence electrons above a closed f shell. The calculation of Ta I is performed to demonstrate the accuracy of the CIPT calculations by comparing with available experimental data.

In Sec. II we briefly discuss the application of the CIPT method, in Sec. III we compare our CIPT calculations for Ta I to experimental results. We present the CIPT calculations for Db I in Sec. IV including calculations of Breit and radiative corrections. Finally, in Sec. V we present optical electric dipole transitions for both Ta I and Db I including calculations of the isotope shift for Db I.

II. CIPT METHOD

The sparse theoretical results for elements $Z = 105$–111 is due to the open $6d$ shell where current methods are not viable. For more than four valence electrons previous many-body methods become too computationally expensive due to the large diagonalization problem. The computational cost is reduced by using a combination of the configuration interaction (CI) and perturbation theory (PT). In this section we will give a brief discussion of our implementation of the CIPT method. For an in depth discussion please refer to Ref. [53].

To generate the single electron wave functions for both Ta I and Db I we use the V^{N-1} approximation (N is the total number of electrons) [54,55]. The Hartree-Fock (HF) calculations are performed for an open-shell atom with a valence s electron removed ($5d^36s$ and $6d^37s$ for Ta and Db, respectively) where single-electron basis states are calculated in the field of the frozen core. We use a B-spline technique [56] with 40 B-spline states of order 9 in each partial wave in a box with radius 40 a_B with partial waves up to $l_{\max} = 4$. Many-electron basis states for the CI calculations are formed by making all possible single and double excitations from reference low-lying configurations.

The wave function for valence electrons has the form of an expansion over single-determinant basis states. It is assumed that the summation in the expansion can be divided in two parts:

$$\Psi(r_1,\dots,r_{N_e}) = \sum_{i=1}^{N_{\rm eff}} c_i\Phi_i(r_1,\dots,r_{N_e}) + \sum_{i=N_{\rm eff}+1}^{N_{\rm total}} c_i\Phi_i(r_1,\dots,r_{N_e}). \quad (1)$$

The first summation goes over the small number of terms which lie low on the energy scale and represent a good approximation for the wave function. The second summation goes over the large number of high-energy terms, however, it represents only a small correction to the wave function. In this case the off-diagonal matrix elements of the CI Hamiltonian between terms from the second summation in Eq. (1) can be neglected and the problem of finding the wave function and corresponding energy is reduced to the matrix eigenvalue problem of the size $N_{\rm eff}$ with modified CI matrix

$$(H^{\rm CI} - EI)X = 0, \quad (2)$$

where I is unit matrix, the vector $X = \{c_1,\dots,c_{N_{\rm eff}}\}$, and the matrix elements of $H^{\rm CI}$ are modified to include a contribution from high states [the second summation in Eq. (1)]:

$$\langle i|H^{\rm CI}|j\rangle \to \langle i|H^{\rm CI}|j\rangle + \sum_k \frac{\langle i|H^{\rm CI}|k\rangle\langle k|H^{\rm CI}|j\rangle}{E-E_k}. \quad (3)$$

Here $|i\rangle \equiv \Phi_i(r_1,\dots,r_{N_e})$, $i, j \leqslant N_{\rm eff}$, $N_{\rm eff} < k \leqslant N_{\rm total}$, $E_k = \langle k|H^{\rm CI}|k\rangle$, and E is the energy of the state of interest. Since this energy is not known in advance, one has to perform iterations

$$[H^{\rm CI}(E^{(i-1)}) - E^{(i)}I]X = 0, \quad (4)$$

where i is the iteration number. To find the initial approximation for the energy one can neglect the modification of the CI matrix [the second term in Eq. (3)]. When convergence is achieved, the solution of Eq. (2) is the exact solution of the full CI problem with off-diagonal matrix elements neglected between high states. In other words, neglecting these matrix elements is the only approximation assumed in the method.

In this work we include the effects of both the Breit interaction [57,58] and quantum electrodynamic (QED) radiative corrections (self-energy and vacuum polarization corrections) [59] for completeness. The Breit interaction which accounts for the magnetic interaction and retardation is included in the zero momentum transfer approximation,

$$\hat{H}^B = -\frac{\boldsymbol{\alpha}_1\cdot\boldsymbol{\alpha}_2 + (\boldsymbol{\alpha}_1\mathbf{n})(\boldsymbol{\alpha}_2\mathbf{n})}{2r}, \quad (5)$$

where $\boldsymbol{\alpha}$ is the Dirac matrix, $\mathbf{r} = r\mathbf{n}$ and r is the distance between electrons denoted by subscripts 1 and 2. Similar to the Coulomb interaction, the Breit interaction (5) leads to the Breit potential V_B, which is added to the HF potential and included into the HF iterations.

The QED radiative corrections due to the Uehling potential V_U and electric and magnetic form-factors V_E and V_g are included via a radiative potential V_R [59],

$$V_R(r) = V_U(r) + V_g(r) + V_E(r). \quad (6)$$

It is also included into the HF procedure. Note that iterating HF equations with Breit and QED potentials V_B and V_R formally lead to the inclusion of nonlinear contributions V_B^2, V_R^2, and so on, which have no physical meaning. We have checks that corresponding contributions are small and cause no problem. On the other hand, iterating the HF equations with V_B and V_R takes into account an important relaxation effect [27] which is first order in V_B or V_R but all order in the Coulomb interaction. This relaxation effect reduces the size of the Breit or QED correction to the energy up to two times [27]. Both the Breit and QED corrections grow with Z faster than first power of Z, therefore it is important to check whether they give significant contributions to the energies of SHE. See Sec. IV for more discussion.

For each level we calculate the Landé g factor and compare it to the nonrelativistic expression

$$g = 1 + \frac{J(J+1) - L(L+1) + S(S+1)}{2J(J+1)}. \quad (7)$$

We treat angular momentum L and spin S as fitting parameters to fit the calculated values of the g factors with the formula (7). This allows us to use the LS notations for atomic states. Note, however, that the SHE states are highly relativistic and strongly mixed and the LS coupling scheme is very approximate.

The ionization potential is obtained by calculating the energy of the ground state of the ion and taking the difference between ground states of the ion and the neutral atom. The same single-electron basis is used for the ion as for the neutral atom.

III. TA I

To demonstrate the accuracy of the CIPT method we compare the theoretical and experimental spectra of Ta I. As Ta lies in the same group but one period lower, we believe the theoretical accuracy of the CIPT Ta spectrum would indicate the accuracy we can expect for Db. Electron states of neutral Ta have an open $5d$ shell, its ground-state configuration is [Xe]$4f^{14}5d^36s^2$. As the $6s$ electrons are easily excited, we should treat the atom as a system with five external electrons. Note that a slightly more complicated atom, tungsten, which has one more external electron, was already successfully studied using the CIPT method [53]. Therefore, we expect similar or better accuracy for Ta. For low-lying even parity states of Ta we used the basis states of the $5d^36s^2$, $5d^46s$, and $5d^5$ configurations in the effective

TABLE I. Comparison of experimental (from Ref. [60]) and CIPT spectra and ionisation potential of Ta I. The experimental excitation energies (E_E) and Landé g factors (g_E) are compared to respective CIPT excitation energies (E_T) and Landé g factors (g_T). The final column is the difference between experimental and theoretical excitation energies $\Delta = E_E - E_T$.

				Experimental		CIPT		
	Configuration	State	J	E_E (cm^{-1})	g_E	E_T (cm^{-1})	g_T	Δ (cm^{-1})
	Even states							
(1)	$5d^36s^2$	^4F	3/2	0.00	0.447	0.00	0.4373	
(2)	$5d^36s^2$	^4F	5/2	2 010	1.031	1 652	1.0336	358
(3)	$5d^36s^2$	^4F	7/2	3 964	1.218	3 175	1.2265	789
(4)	$5d^36s^2$	^4F	9/2	5 621	1.272	4 679	1.3066	942
(5)	$5d^36s^2$	^4P	1/2	6 049	2.454	6 017	2.4022	32
	Odd states							
(6)	$5d^36s6p$	$^6G^\circ$	3/2	17 385		17 599	0.1719	−214
(7)	$5d^36s6p$	$^2F^\circ$	5/2	17 994	0.732	18 225	0.7955	−231
(8)	$5d^26s^26p$	$^4D^\circ$	1/2	18 505	0.172	18 629	0.0716	−124
(9)	$5d^36s6p$	$^6G^\circ$	5/2	19 178	0.851	19 393	0.8551	−123
(10)	$5d^26s^26p$	$^4D^\circ$	3/2	19 658	1.018	19 724	0.9389	−66
(11)	$5d^26s^26p$	$^2S^\circ$	1/2	20 340	1.956	20 574	2.0278	−233
(12)	$5d^36s6p$	$^6G^\circ$	7/2	20 560	1.194	20 463	1.1394	−97
(13)	$5d^26s^26p$	$^2D^\circ$	3/2	20 772	0.812	20 796	0.8124	−24
(14)	$5d^26s^26p$	$^4D^\circ$	5/2	21 168		21 358	1.2117	−190
(15)	$5d^36s6p$	$^4F^\circ$	3/2	21 855	0.666	22 132	0.6773	−277
(16)	$5d^26s^26p$	$^2D^\circ$	5/2	22 047	1.179	21 875	1.0838	172
(17)	$5d^26s^26p$	$^4G^\circ$	7/2	22 381	1.060	22 276	1.0377	105
(18)	$5d^36s6p$	$^6G^\circ$	9/2	22 682	1.231	22 285	1.2677	397
(19)	$5d^36s6p$	$^6F^\circ$	1/2	23 355	−0.320	23 680	−0.2689	−325
(20)	$5d^36s6p$	$^4F^\circ$	5/2	23 363	1.078	23 381	1.0766	−18
(21)	$5d^26s^26p$	$^4D^\circ$	7/2	23 927	1.326	23 572	1.3256	355
(22)	$5d^36s6p$	$^6F^\circ$	3/2	24 243	1.126	24 463	1.1018	−220
(23)	$5d^36s6p$	$^6D^\circ$	1/2	24 517	2.888	24 907	2.9261	−390
(24)	$5d^36s6p$	$^6D^\circ$	3/2	24 739	1.620	25 143	1.6808	−404
(25)	$5d^36s6p$	$^4F^\circ$	7/2	24 982	1.235	24 922	1.2590	60
(26)	$5d^36s6p$	$^6G^\circ$	11/2	25 009	1.302	24 528	1.3366	481
(27)	$5d^36s6p$	$^6F^\circ$	5/2	25 181	1.239	25 267	1.2573	−86
(28)	$5d^36s6p$	$^6G^\circ$	9/2	25 186		24 733	1.2540	453
(29)	$5d^36s6p$	$^4D^\circ$	1/2	25 513	0.028	25 697	0.0319	−184
(30)	$5d^36s6p$	$^4F^\circ$	9/2	25 926	1.292	25 509	1.2970	417
(31)	$5d^26s^26p$	$^4\mathrm{P}^\circ$	5/2	26 220	1.338	26 298	1.2923	−78
(32)	$5d^36s6p$	$^4D^\circ$	3/2	26 364	1.393	26 678	1.2676	−314
(33)	$5d^36s6p$	$^6F^\circ$	7/2	26 586	1.356	26 299	1.315	287
(34)	$5d^26s^26p$	$^4P^\circ$	3/2	26 590	1.576	26 759	1.6833	−169
(35)	$5d^36s6p$	$^6D^\circ$	5/2	26 795	1.416	26 815	1.4086	−20
(36)	$5d^26s^26p$	$^4P^\circ$	1/2	26 866	2.650	27 094	2.6189	−228
(37)	$5d^36s6p$	$^4F^\circ$	7/2	26 960	1.223	26 787	1.2390	173
(38)	$5d^36s6p$	$^6F^\circ$	9/2	27 733	1.390	27 279	1.3590	454
(39)	$5d^36s6p$	$^4D^\circ$	7/2	27 781	1.374	27 643	1.4658	138
(40)	$5d^36s6p$	$^6G^\circ$	11/2	27 783	1.351	27 376	1.350	407
(41)	$5d^36s6p$	$^4D^\circ$	5/2	28 134	1.394	28 337	1.3665	−203
(42)	$5d^36s6p$	$^4G^\circ$	7/2	28 183	1.115	27 970	1.0421	213
(43)	$5d^36s6p$	$^2P^\circ$	3/2	28 689	1.356	28 693	1.3052	−4
(44)	$5d^36s6p$	$^6D^\circ$	9/2	28 767	1.337	28 414	1.4106	353
(45)	$5d^36s6p$	$^6F^\circ$	5/2	28 862	1.247	28 868	1.2678	−6
(46)	$5d^36s6p$	$^6D^\circ$	1/2	29 902	2.994	30 323	2.9971	−421
	Ta I ionisation potential							
(47)	$5d^36s$	$5F$	1	60 891	0.000	61 073	0.0235	−182

CI matrix. All other configurations, which were obtained by exciting one or two electrons from these configurations, were included perturbatively. Similarly for the odd parity states we use the states of the $5d^36s6p$, $5d^26s^26p$ configurations in the effective CI matrix, while other configurations are included perturbatively.

In Table I we present the comparison between experimental excitation energies and g factors and those calculated by the CIPT method. We present a significant number of odd parity states to demonstrate the accuracy of these states, particularly towards the end of the optical region. This is because the most promising measurements are strong optical electric dipole ($E1$) transitions between the ground state and excited states of different parity. It is important to include as many of these transitions as possible. To identify the correct states for comparison to the experiment we use the experimental and theoretical Landé g factors. When experimental g factors were not available we use the next sequential state in the theoretical calculations. There is excellent agreement between the experimental and CIPT g factors with maximum difference between the theory and experiment $\Delta g \approx 0.1$. This is sufficient accuracy for identification of the states.

There is good agreement between the experimental and theoretical excitation energies particularly for the low-lying odd parity states which are important for measuring the electric dipole transitions (see Sec. V). For the odd parity states the largest discrepancy in energy was $\Delta = 453$ cm^{-1} with most states having $|\Delta| \approx 100$–400 cm^{-1}. The main source of the difference between theory and experiment is incomplete treatment of the correlations, which mostly comes from two factors. We neglect core valence correlations and off-diagonal matrix elements between highly excited states. This is the price we have to pay to be able to perform the calculations for a complicated system with five external electrons. There are some smaller factors, like the cutting basis at $l_{\max} = 4$, ignoring triple excitations, and so on. For the CIPT calculations of the Db I spectrum we expect a similar accuracy as seen in Ta I due to the similar electronic structure.

IV. DB I

Dubnium was first synthesized in 1968 and the current longest living isotope is ^{268}Db with a half-life of ≈30 hrs [61,62]. This long lifetime relative to other SHEs makes future experiments promising. There is limited experimental and theoretical data for Db with the majority being chemical properties [61,63]. An estimation of the ionization potential has been performed for Db in Ref. [50] using a relativistic Hartree-Fock method with semi-empirical corrections introduced to simulate the effect of correlations.

For the CIPT calculations of Db I we use the same parameters as for the Ta I calculations in Sec. III. In the V^{N-1} approximation discussed in Sec. II we remove a $7s$ electron in the initial Hartree-Fock calculations and in the calculation of the single-electron basis states. The Db I ground state is [Rn]$5f^{14}6d^37s^2$, which is similar to Ta I with different principle quantum numbers. For calculation of the even parity states we populate the effective CI matrix with the states of the $6d^37s^2$, $6d^47s$, and $6d^5$ configurations. All higher states are obtained through single and double excitations of these states and are included perturbatively. Similarly for the states of odd parity the effective matrix contains states of the $6d^37s7p$, $6d^27s^27p$, and $6d^47p$ configurations. Other configurations are included perturbatively. For the ion we use the states of the $6d^37s$, $6d^27s^2$, and $6d^4$ configurations. Both Breit and radiative corrections are expected to be larger in SHE compared to lighter elements and therefore are included in Table II. In Table II we present the excitation energies of Db using the CIPT method. To demonstrate the affect of Breit and QED corrections we performed four separate calculations, first with no Breit or QED corrections, second with only the Breit correction included, then with QED included but no Breit, and finally, with both corrections included (see Table II).

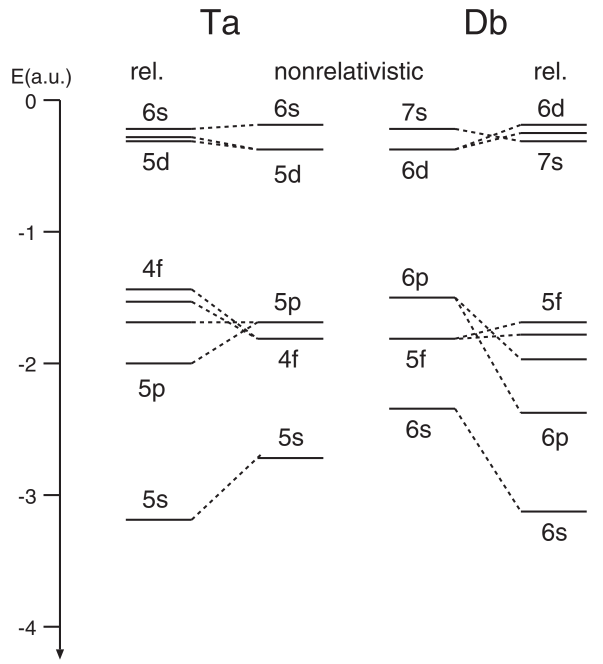

FIG. 1. Hartree-Fock energies of upper core states of Ta and Db calculated in nonrelativistic and relativistic approximations.

Comparing the Db I spectrum in Table II to the Ta I spectrum in Table I we see there are some notable differences. While the order of even parity states has remained the same relative to each other, the order of the odd states has been significantly altered with the first $2F^o_{5/2}$ state being significantly lowered in the spectrum. Another thing to note is that the odd parity excitations are typically $6d \rightarrow 7p$ as opposed to the Ta excitation $6s \rightarrow 6p$. This can be explained by relativistic effects where the $7s$ electrons are more tightly bound than the $6d$ electrons in contrast to the $5d$ and $6s$ electrons in Ta [48]. These relativistic effects also cause the $6d$ electron to be ionized in Db instead of the $7s$ electron. This may result in significantly different chemical properties in Db compared to Ta.

To understand the difference between the atoms it is instructive to look at the Hartree-Fock energies and electron densities calculated in nonrelativistic and relativistic approximations. Figure 1 shows energies of the upper core states of Ta and Db. The spectra are very similar. Relativistic energy shifts are larger for Db as expected and the most noticeable difference cause by this shift is the change of the order of the $6d$ and $7s$

TABLE II. Spectrum for the low-lying energy levels of Db I and Db II using the CIPT method. Here E_{NC} are the excitation energies when neither Breit nor radiative corrections are included in the calculations, Δ_B and Δ_R are the changes in energy from E_{NC} when Breit and radiative corrections are included, respectively. The final energy E is the excitation spectrum when both Breit and radiative corrections are included *ab initio*. The accuracy of these levels is expected to be similar to Ta I presented in Table I.

				Excitation energy				
	Major Configuration	State	J	CIPT with no Breit or QED E_{NC} (cm^{-1})	Breit correction Δ_B (cm^{-1})	QED corrections Δ_R (cm^{-1})	Total E (cm^{-1})	Landé g factor
	Even States							
(1)	$6d^37s^2$	^4F	3/2	0	0	0	0	0.554
(2)	$6d^37s^2$	^4F	5/2	4 072	−77	21	4 016	1.043
(3)	$6d^37s^2$	^2F	7/2	6 595	−100	31	6 527	1.170
(4)	$6d^37s^2$	^2S	1/2	7 691	−73	16	7 634	2.058
(5)	$6d^37s^2$	^4G	9/2	8 076	−92	33	8 017	1.191
	Odd States							
(6)	$6d^27s^27p$	$^2F^o$	5/2	6 255	213	123	6 591	0.739
(7)	$6d^27s^27p$	$^2D^o$	3/2	11 240	156	87	11 483	0.633
(8)	$6d^27s^27p$	$^2P^o$	1/2	12 642	140	84	12 869	1.308
(9)	$6d^27s^27p$	$^4G^o$	7/2	13 645	116	147	13 909	1.023
(10)	$6d^27s^27p$	$^4F^o$	5/2	13 873	113	132	14 117	1.067
(11)	$6d^27s^27p$	$^2P^o$	1/2	14 516	96	88	14 705	0.995
(12)	$6d^27s^27p$	$^6F^o$	3/2	14 572	105	96	14 772	1.111
(13)	$6d^27s^27p$	$^4F^o$	5/2	17 493	78	76	17 647	1.111
(14)	$6d^27s^27p$	$^4G^o$	9/2	18 596	80	144	18 820	1.145
(15)	$6d^37s7p$	$^2D^o$	3/2	19 379	62	−3	19 438	0.701
(16)	$6d^27s^27p$	$^4F^o$	7/2	20 462	53	134	20 649	1.203
(17)	$6d^27s^27p$	$^6F^o$	3/2	21 706	56	50	21 811	1.073
(18)	$6d^27s^27p$	$^4D^o$	1/2	22 123	72	93	22 284	0.078
(19)	$6d^27s^27p$	$^4F^o$	5/2	22 204	35	54	22 292	1.110
(20)	$6d^27s^27p$	$^2D^o$	3/2	23 003	39	22	23 067	0.697
(21)	$6d^27s^27p$	$^2F^o$	7/2	23 221	37	133	23 390	1.102
(22)	$6d^37s7p$	$^4F^o$	5/2	23 910	4	−2	23 913	0.948
(23)	$6d^27s^27p$	$^2P^o$	3/2	24 622	2	119	24 743	1.372
(24)	$6d^27s^27p$	$^2G^o$	9/2	24 915	27	133	25 074	1.111
(25)	$6d^37s7p$	$^2F^o$	7/2	25 458	9	17	25 480	1.152
(26)	$6d^27s^27p$	$^4F^o$	5/2	25 510	5	73	25 589	1.031
(27)	$6d^27s^27p$	$^2F^o$	7/2	26 538	−4	78	26 612	1.172
(28)	$6d^27s^27p$	$^2S^o$	1/2	27 435	−10	49	27 479	1.663
(29)	$6d^27s^27p$	$^2F^o$	7/2	27 662	−23	24	27 666	1.128
(30)	$6d^27s^27p$	$^4D^o$	3/2	27 589	−5	114	27 697	1.147
(31)	$6d^27s^27p$	$^4G^o$	9/2	27 885	−13	118	27 990	1.173
(32)	$6d^27s^27p$	$^2D^o$	5/2	28 162	−25	75	28 211	1.130
(33)	$6d^27s^27p$	$^4P^o$	3/2	29 183	1	74	29 259	1.659
(34)	$6d^27s^27p$	$^4G^o$	11/2	29 669	−45	103	29 669	1.254
(35)	$6d^37s7p$	$^6G^o$	9/2	29 946	−75	−87	29 784	1.254
(36)	$6d^27s^27p$	$^6F^o$	5/2	29 734	−25	174	29 821	1.343
(37)	$6d^37s7p$	$^4D^o$	1/2	29 886	−24	−33	29 832	0.220
(38)	$6d^27s^27p$	$^2F^o$	7/2	30 474	−29	97	30 541	1.161
	Db II states							
(39)	$6d^27s^2$	^3F	2	56 546	48	139	56 733	0.731
(40)	$6d^27s^2$	^3S	0	62 673	−13	119	62 778	0.000
(41)	$6d^27s^2$	^3F	3	62 952	−45	176	63 083	1.083
(42)	$6d^27s^2$	^3D	2	65 122	−62	120	65 179	1.250
(43)	$6d^27s^2$	^3P	1	65 587	−79	113	65 620	1.467
(44)	$6d^27s^2$	^5G	4	67 466	−83	189	67 572	1.120

states which leads to the change of the dominant configurations in low odd states of Db as discussed above. However, the absolute shift of the energies is small. It changes the order of the states because they are very close in the nonrelativistic calculations. This change in the Hartree-Fock spectra caused by relativistic effects suggests that the differences in the spectra of neutral Ta and Db are mostly due to relativistic effects while correlation corrections are similar. This means that the

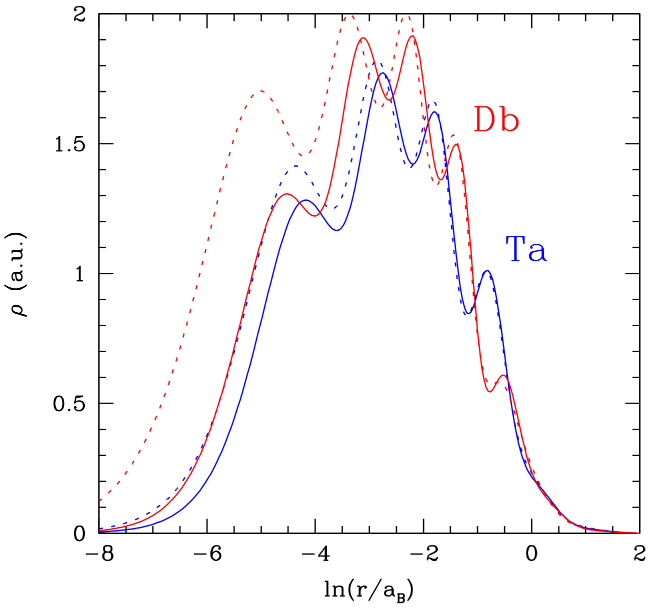

FIG. 2. Electron density normalized to one ($\int \rho dV = 1$) of Db and Ta calculated in nonrelativistic (solid line) and relativistic (dotted line) approximations.

accuracy of the calculations should also be similar for Ta and Db. This can be further illustrated by comparing the electron densities of the atoms calculated in nonrelativistic and relativistic approximations (see Fig. 2). Examining the densities one can see the following: (a) There are four peaks for Ta and five for Db. They correspond to shells with principal quantum numbers from 1 to 4 for Ta and 1 to 5 for Db. Electrons in higher shells are distributed over larger distances and their density does not form a peak. (b) Relativistic effects pull inner electrons towards the nucleus but have little effect on outer electrons. (c) The densities at large distances ($r > a_B$), where external electrons are located, are very similar. This is another indication that correlations are likely to be similar. To check this we performed another test. We compared the contribution of high-energy states [the second term in Eq. (3)] to the energies of Ta and Db. It turns out that the corrections to the energies of even states of Ta and Db differ by 2% only while corrections to the energies of odd states of Db about 30% larger than those of Ta. This means the uncertainty in the calculations for these states might also be larger for Db. Therefore, it seems to be reasonable to increase the estimated uncertainty from ~400 cm^{-1} for Ta to ~500 cm^{-1} for Db.

From Table II we see that the effect of both the Breit interaction (Δ_B) and radiative corrections (Δ_R) is small and lies within the accuracy of our CIPT method. As it was discussed in the previous section, the main source of the uncertainty of the calculations comes from incomplete treatment of the correlations and it is <500 cm^{-1} for Ta. It is expected to be similar for Db. On the other hand, the maximum value of the sum of Breit and QED corrections for Db is ~300 cm^{-1} while for most of the states it is <200 cm^{-1} (see Table II). It is interesting that the Breit and QED effects do not correlate with each other. This can be seen by summing the two corrections and the calculated energy with no corrections included (E_{NC}). This energy is very close to states in the spectrum which include both corrections simultaneously,

$$E \approx E_{NC} + \Delta_B + \Delta_R.$$

Including both Breit and QED effects simultaneously will introduce new terms which are second order in perturbations of the interactions. Since both corrections are small these new terms will be negligible. To test the consistency of our method we calculated the spectrum of Db I using the V^{N-1} approach removing a $6d$ electron for the frozen core potential. In these calculations we obtained a similar spectrum within the accuracy of our calculations.

During the completion of our work another paper on the calculation of the Db spectrum appeared [64]. The calculations are done with a different implementation of a very similar method. The difference between the results of two papers seems to be larger than the uncertainty of our calculations. However, if we accept the difference between theory and experiment for Ta in Ref. [64] as an estimation of the uncertainty of their calculations, the results are consistent.

We are not aware of any other calculations of the Db spectrum apart from the calculations of IP. Our value 56744 cm^{-1} is in good agreement with the Hartree-Fock number 55 000(7000) cm^{-1} [50] and coupled cluster number 55 590 cm^{-1} [65]. Note that the IP of Db is significantly smaller than the IP of Ta [IP(Ta) = 60891 cm^{-1}, see previous section] which is another indication of possible different chemical properties.

V. ELECTRIC DIPOLE TRANSITIONS AND ISOTOPE SHIFT

Due to the current low production rate of dubnium and other SHEs, broad spectroscopic scans are unfeasible for current experimental methods. Therefore, experimental searches need to be assisted with theoretical predictions of the strongest lines specifically for optical electric dipole ($E1$) transitions. In this work we calculate and present the $E1$ transition amplitudes for the major optical transitions between the ground state and the lowest-lying odd-parity states for each Ta I and Db I. It should be noted that there is no published data for the $E1$ transitions for either Ta I or Db I and therefore we present the $E1$ transition amplitudes (A_{E1}) and transition probabilities (T_{E1}) for both atoms.

To calculate the $E1$ transition amplitudes A_{E1} we use the self-consistent random-phase approximation (RPA) to simulate the atom in an external electromagnetic field. This results in an effective electric dipole field for the electrons. The $E1$ transition amplitude for a transition between states a and b is given by $A_{E1} = \langle b||\hat{D} + \delta V||a\rangle$ where $|a\rangle$ and $|b\rangle$ are the many electron wave functions calculated in the CIPT method above, $\hat{D}$ is the electric dipole operator acting on external electrons, δV is the correction to the self-consistent Hartree-Fock potential of the atomic core caused by photon electric field. For a more in-depth discussion on this method refer to Ref. [66].

The $E1$ transition rates are calculated using (in atomic units)

$$T_{E1} = \frac{4}{3}(\alpha\omega)^3 \frac{A_{E1}^2}{2J+1},$$

TABLE III. Allowed electric dipole transitions between the ground states of Db I ($^4F_{3/2}$) and Ta I ($^4F_{3/2}$) and their low-lying odd parity states. The numbers next to the states correspond to the numbered spectra in Tables I and II. The transition amplitudes A_{E1} are in atomic units. For the Db I transitions we include the associated isotope shift parameters a and F. The isotope shift calculation was performed for ^{268}Db ($\langle r^2\rangle_{268} = 36.770$ fm^2) and ^{289}Db ($\langle r^2\rangle_{289} = 38.470$ fm^2).

	Ta I				Db I				
	State	A_{E1} (a.u)	T_{E1} (10^6 s^{-1})		State	A_{E1} (a.u)	T_{E1} (10^6 s^{-1})	a (cm^{-1})	F (cm^{-1}/fm^2)
(6)	$^6G^o_{3/2}$	−0.270	0.194	(6)	$^2F^o_{5/2}$	0.631	0.0385	32.16	3.11
(7)	$^2F^o_{5/2}$	0.214	0.090	(7)	$^2D^o_{3/2}$	1.53	1.80	18.70	1.81
(8)	$^4D^o_{1/2}$	−0.641	2.64	(8)	$^2P^o_{1/2}$	0.558	0.672	−3.42	−0.33
(9)	$^6G^o_{5/2}$	−0.434	0.449	(10)	$^4F^o_{5/2}$	−0.531	0.268	27.33	2.64
(10)	$^4D^o_{3/2}$	0.149	0.0856	(11)	$^2P^o_{1/2}$	0.384	0.476	15.78	1.52
(11)	$^2S^o_{1/2}$	−0.107	0.0973	(12)	$^6F^o_{3/2}$	0.180	0.0527	14.93	1.44
(13)	$^2D^o_{3/2}$	0.495	1.12	(13)	$^4F^o_{5/2}$	−0.339	0.213	8.39	0.81
(14)	$^4D^o_{5/2}$	−0.200	0.128	(15)	$^2D^o_{3/2}$	−0.343	0.437	−18.84	−1.82
(15)	$^4F^o_{3/2}$	−0.360	0.688	(17)	$^6F^o_{3/2}$	1.22	7.85	−0.33	−0.03
(16)	$^2D^o_{5/2}$	0.069	0.0160	(18)	$^4D^o_{1/2}$	0.0968	0.105	13.58	1.31
(19)	$^6F^o_{1/2}$	0.019	0.00446	(19)	$^4F^o_{5/2}$	−0.163	0.0996	−1.54	−0.51
(20)	$^4F^o_{5/2}$	−0.094	0.0381	(20)	$^2D^o_{3/2}$	0.784	3.83	−4.88	−0.47
(22)	$^6F^o_{3/2}$	0.007	0.000412	(22)	$^4F^o_{5/2}$	−1.01	4.70	−19.24	−1.86
(23)	$^6D^o_{1/2}$	−0.073	0.0795	(23)	$^2P^o_{3/2}$	−0.150	0.173	16.75	1.62
(24)	$^6D^o_{3/2}$	−0.249	0.477	(26)	$^4F^o_{5/2}$	−0.890	4.49	6.22	0.60
(27)	$^6F^o_{5/2}$	−0.356	0.683	(28)	$^2S^o_{1/2}$	−0.570	6.83	−4.42	−0.43
(29)	$^4D^o_{1/2}$	0.282	1.34	(30)	$^4D^o_{3/2}$	−0.114	0.139	16.04	1.55
(31)	$^4P^o_{5/2}$	0.202	0.248	(32)	$^2D^o_{5/2}$	0.228	0.393	3.31	0.32
(32)	$^4D^o_{3/2}$	0.405	1.53	(33)	$^4P^o_{3/2}$	−0.388	2.01	6.68	0.64
(34)	$^4P^o_{3/2}$	−0.063	0.0377	(36)	$^6F^o_{5/2}$	−0.0174	0.00270	14.86	1.44
(35)	$^6D^o_{5/2}$	0.338	0.741	(37)	$^4D^o_{1/2}$	1.49	59.7	−28.14	−2.72
(36)	$^4P^o_{1/2}$	−0.066	0.0859						
(41)	$^6D^o_{5/2}$	−0.278	0.583						
(43)	$^2P^o_{1/2}$	−0.295	1.04						

where J is the angular momentum of the odd parity state, α is the fine-structure constant, and ω is the frequency of the transitions in atomic units. All calculations obey the selection rules for $E1$ transitions, a change in parity and change in angular momenta $|\Delta J| \leqslant 1$. We present the $E1$ transitions for Ta I and Db I in Table III.

For Db from Table III we see that the transition between the ground state and the odd parity state $^4F_{3/2} \rightarrow {}^4D^o_{1/2}$ with has the largest transition rate $T_{E1} = 59.7 \times 10^6$ s^{-1} with an energy difference 29 886 cm^{-1}. The rate of this transition is an order of magnitude lower than the recently measured transition in Ref. [6] and calculated in Refs. [16,21,35], however. the level is at a similar energy, which may be promising for future experiments on Db. Other promising transitions from the ground state are to states (7), (17), (20), (22), (33), although the rate of these transition are an order of magnitude lower. Large $E1$ amplitudes can probably be found when configuration mixing allows for a significant contribution of the $7p \rightarrow 7s$ transition as opposed to the $7p \rightarrow 6d$ transition. This is especially clear for the $^4F_{3/2} \rightarrow {}^4D^o_{1/2}$ transition considered above.

Finally, we calculate isotope shift for Db. Isotope shift is important since it helps to obtain information about nuclei of SHE when frequencies of the transitions are measured for several isotopes. It can also be used to predict the spectra of other isotopes, in particular, the spectrum of the hypothetically stable neutron-rich isotopes with "magic" number of neutrons $N = 184$. This may help in search for such isotopes.

Isotope shift of SHE elements is strongly dominated by volume shift (also known as "field shift" in literature). We calculate it by varying the nuclear radius in computer codes. We present results in two different forms. The first is given by [67]

$$\delta\nu = E_2 - E_1 = a\big(A_2^{1/3} - A_1^{1/3}\big),$$

where A_1 and A_2 are atomic numbers for two isotopes ($A_2 > A_1$) and a is the parameter which comes from the calculations. This form is convenient for the prediction of the spectra of heavier isotopes. It is motivated by the relativistic dependence of the volume shift on the nuclear radius, R_N, which is proportional to $R_N^{2\gamma}$ where $\gamma = \sqrt{1-(Z\alpha)^2}$. For Db $R_N^{2\gamma} \approx R_N^{1.28}$ and using the large-scale trend for nuclear radii $R_N \propto A^{1/3}$ the volume shift can be approximated by $\propto A^{1/3}$. This nuclear radius approximation is valid for large-scale trends in A where nuclear shell fluctuations are suppressed [67,68], this is applicable for our Db I calculations as A_1 and A_2 are not neighboring isotopes.

Another form for the isotope shift is the standard formula related to the change of atomic frequency to the change of nuclear radius

$$\delta\nu = F\delta\langle r^2\rangle.$$

This formula is convenient for the extraction of the nuclear radius change from the isotope shift measurements. The values of the a and F parameters for strong electric dipole transitions of Db are presented in Table III.

VI. CONCLUSION

We calculate low-lying energy levels, electric dipole transition amplitudes, and isotope shift for superheavy element dubnium. Similar CIPT calculations for its lighter analog Ta indicate that the uncertainty of the results for the energies of Db is unlikely to exceed 500 cm^{-1}. Db is the first SHE with open $6d$ shell which is studied with the recently developed CIPT method.

ACKNOWLEDGMENTS

We thank Julian Berengut, Daniel Czapski, and Amy Geddes for useful discussions. This work was funded, in part, by the Australian Research Council under Grant No. DP150101405.

---

[1] Y. Oganessian, Eur. Phys. J. A **42**, 361 (2009).
[2] J. H. Hamilton, S. Hofmann, and Y. T. Oganessian, Annu. Rev. Nucl. Part. Sci **63**, 383 (2013).
[3] Y. T. Oganessian, V. K. Utyonkov, Y. V. Lobanov, F. S. Abdullin, and A. N. Polyakov, Nucl. Phys. A **734**, 109 (2004).
[4] M. Leino, EPJ Web Conf. **131**, 01002 (2016).
[5] Y. Oganessian, Acta Phys. Pol. B **43**, 167 (2012).
[6] M. Laatiaoui, W. Lauth, H. Backe, M. Block, and D. Ackermann, Nature **538**, 495 (2016).
[7] T. K. Sato, M. Asai, A. Borschevsky, T. Stora, N. Sato, Y. Kaneya, and K. Tsukada, Nature **520**, 209 (2015).
[8] M. Laatiaoui, H. Backe, M. Block, P. Chhetri, F. Lautenschläger, W. Lauth, and T. Walther, Hyperfine Interact. **227**, 69 (2014).
[9] M. Laatiaoui, EPJ Web Conf. **131**, 05002 (2016).
[10] R. Ferrer *et al.*, Nat. Commun. **8**, 14520 (2017).
[11] I. Lindgren and J. Morrison, *Atomic Many-Body Theory*, 2nd ed. (Springer-Verlag, Berlin, 1986).
[12] S. A. Blundell, W. R. Johnson, and J. Sapirstein, Phys. Rev. A **43**, 3407 (1991).
[13] V. A. Dzuba, V. V. Flambaum, and M. G. Kozlov, Phys. Rev. A **54**, 3948 (1996).
[14] V. A. Dzuba, V. V. Flambaum, and O. P. Sushkov, Phys. Lett. A **140**, 493 (1989).
[15] I. P. Grant and H. M. Quiney, Adv. At. Mol. Phys. **23**, 37 (1988).
[16] Y. Liu, R. Hutton, and Y. Zou, Phys. Rev. A **76**, 062503 (2007).
[17] J. P. Desclaux and B. Fricke, J. Phys. **41**, 943 (1980).
[18] E. Eliav, U. Kaldor, and Y. Ishikawa, Phys. Rev. Lett. **74**, 1079 (1995).
[19] S. Fritzsche, C. Z. Dong, F. Koike, and A. Uvarov, Eur. Phys. J. D **45**, 107 (2007).
[20] Y. Zou and C. F. Fischer, Phys. Rev. Lett. **88**, 183001 (2002).
[21] A. Borschevsky, E. Eliav, M. J. Vilkas, Y. Ishikawa, and U. Kaldor, Eur. Phys. J. D **45**, 115 (2007).
[22] W. C. Martin and J. Sugar, Phys. Rev. A **53**, 1911 (1996).
[23] N. S. Mosyagin, I. I. Tupitsyn, and A. V. Titov, Radiochemistry **52**, 394 (2010).
[24] V. A. Dzuba, M. S. Safronova, and U. I. Safronova, Phys. Rev. A **90**, 012504 (2014).
[25] E. Eliav, S. Fritzsche, and U. Kaldor, Nucl. Phys. A **944**, 518 (2015).
[26] A. Borschevsky, E. Eliav, M. J. Vilkas, Y. Ishikawa, and U. Kaldor, Phys. Rev. A **75**, 042514 (2007).
[27] V. A. Dzuba and V. V. Flambaum, Hyperfine Interact. **237**, 160 (2016).
[28] V. Pershina, A. Borschevsky, E. Eliav, and U. Kaldor, J. Chem. Phys. **128**, 024707 (2008).
[29] C. S. Nash, J. Phys. Chem. A **109**, 3493 (2005).
[30] A. Landau, E. Eliav, Y. Ishikawa, and U. Kaldor, J. Chem. Phys. **114**, 2977 (2001).
[31] A. Borschevsky, L. F. Pašteka, V. Pershina, E. Eliav, and U. Kaldor, Phys. Rev. A **91**, 020501 (2015).
[32] C. Thierfelder, B. Assadollahzadeh, P. Schwerdtfeger, S. Schäfer, and R. Schäfer, Phys. Rev. A **78**, 052506 (2008).
[33] V. Pershina, A. Borschevsky, E. Eliav, and U. Kaldor, J. Phys. Chem. A **112**, 13712 (2008).
[34] T. H. Dinh and V. A. Dzuba, Phys. Rev. A **94**, 052501 (2016).
[35] P. Indelicato, J. P. Santos, S. Boucard, and J. P. Desclaux, Eur. Phys. J. D **45**, 155 (2007).
[36] T. H. Dinh, V. A. Dzuba, and V. V. Flambaum, Phys. Rev. A **78**, 062502 (2008).
[37] E. Eliav, U. Kaldor, Y. Ishikawa, M. Seth, and P. Pyykkö, Phys. Rev. A **53**, 3926 (1996).
[38] Y. J. Yu, C. Z. Dong, J. G. Li, and B. Fricke, J. Chem. Phys. **128**, 124316 (2008).
[39] A. Landau, E. Eliav, Y. Ishikawa, and U. Kaldor, J. Chem. Phys. **115**, 2389 (2001).
[40] I. S. Lim, P. Schwerdtfeger, B. Metz, and H. Stoll, J. Chem. Phys. **122**, 104103 (2005).
[41] T. H. Dinh, V. A. Dzuba, V. V. Flambaum, and J. S. M. Ginges, Phys. Rev. A **78**, 054501 (2008).
[42] T. H. Dinh, V. A. Dzuba, V. V. Flambaum, and J. S. M. Ginges, Phys. Rev. A **78**, 022507 (2008).
[43] G. Gaigalas, E. Gaidamauskas, Z. Rudzikas, N. Magnani, and R. Caciuffo, Phys. Rev. A **81**, 022508 (2010).
[44] A. Borschevsky, V. Pershina, E. Eliav, and U. Kaldor, Phys. Rev. A **87**, 022502 (2013).
[45] L. V. Skripnikov, N. S. Mosyagin, and A. V. Titov, Chem. Phys. Lett. **555**, 79 (2013).
[46] V. A. Dzuba, Phys. Rev. A **88**, 042516 (2013).
[47] J. S. M. Ginges and V. A. Dzuba, Phys. Rev. A **91**, 042505 (2015).
[48] P. Schwerdtfeger, L. F. Pašteka, A. Punnett, and P. O. Bowman, Nucl. Phys. A **944**, 551 (2015).
[49] A. Türler and V. Pershina, Chem. Rev. **113**, 1237 (2013).
[50] V. A. Dzuba, Phys. Rev. A **93**, 032519 (2016).
[51] E. Johnson, V. Pershina, and B. Fricke, J. Phys. Chem. A **103**, 8458 (1999).
[52] E. Johnson, B. Fricke, T. Jacob, C. Z. Dong, S. Fritzsche, and V. Pershina, J. Chem. Phys. **116**, 1862 (2002).
[53] V. A. Dzuba, J. C. Berengut, C. Harabati, and V. V. Flambaum, Phys. Rev. A **95**, 012503 (2017).

[54] H. P. Kelly, Phys. Rev. **136**, B896 (1964).

[55] V. A. Dzuba, Phys. Rev. A **71**, 032512 (2005).

[56] W. R. Johnson, S. A. Blundell, and J. Sapirstein, Phys. Rev. A **37**, 307 (1988).

[57] G. Breit, Phys. Rev. **34**, 375 (1929).

[58] J. B. Mann and W. R. Johnson, Phys. Rev. A **4**, 1 (1971).

[59] V. V. Flambaum and J. S. M. Ginges, Phys. Rev. A **72**, 052115 (2005).

[60] A. Kramida, Yu. Ralchenko, J. Reader, and NIST ASD Team, NIST Atomic Spectra Database (ver. 5.5.6) [Online]. Available: `https://physics.nist.gov/asd` [2018, June 2] (National Institute of Standards and Technology, Gaithersburg, MD, 2018).

[61] B. M. Schädel, *The Chemistry of Superheavy Elements* (Springer, New York, 2012), Vol. 604.

[62] Y. T. Oganessian *et al.*, Phys. Rev. C **72**, 034611 (2005).

[63] B. Fricke, Superheavy elements a prediction of their chemical and physical properties, in *Recent Impact of Physics on Inorganic Chemistry, Structure and Bonding, Vol. 21* (Springer, Berlin, 1975).

[64] A. J. Geddes, D. A. Czapski, E. V. Kahl, and J. C. Berengut, arXiv:1805.06615 (2018).

[65] A. Borschevsky (private communication).

[66] V. A. Dzuba, V. V. Flambaum, and S. Schiller, Phys. Rev. A **98**, 022501 (2018).

[67] V. A. Dzuba, V. V. Flambaum, and J. K. Webb, Phys. Rev. A **95**, 062515 (2017).

[68] I. Angeli and K. P. Marinova, At. Data Nucl. Data Tables **99**, 69 (2013).